

Cryo-TEMPO

Algorithm Theoretical Basis Document

Inland Water



Prepared by	: B. Calmettes & J. Renou	11/05/2022
Checked by	: S. Hendricks	20/7/2022
Approved by	:	

Change Log

Issue	Author	Affected Section	Change	Status
0	B. Calmettes	All	Document Creation	Complete
1.1	B. Calmettes	All	Version 1 Content	Complete
1.2	B. Calmettes	All	Version 1 Revisions	In Review
2.1	J. Renou			

Acronyms and Abbreviations

AD	Applicable Document	REAPER	RÉprocessing of Altimeter Products for ERs
ADT	Absolute Dynamic Topography	RFW	Request for Waiver
ATM	Airborne Topographic Mapper	RMSD	Root mean square difference
AWI	Alfred Wegener Institute	SAR	Synthetic Aperture Radar
C3S	Copernicus Climate Change Service	SARIn	Synthetic Aperture Radar Interferometric
CCI	Climate Change Initiative	SL	Science Lead
CCN	Contract Change Notice	SLA	Sea Level Anomaly
CLS	Collecte Localisation Satellites	SoW	Statement of Work
CNES	Centre National des Etudes Spatiales (French Space Agency)	SS	Shepherd Space
CNR	Consiglio Nazionale delle Ricerche	TCOG	Threshold Centre of Gravity
CPOM	Centre for Polar Observation & Modelling	TDP	Thematic Data Product
CR	Change Request	TFMRA	Threshold First Maximum Retracker Algorithm
CRISTAL	Copernicus Polar Ice and Snow Topography Altimeter	TUG	Thematic User Group
CryoVEx	Cryosat Validation Experiment (field campaigns)	UCL	University College London
DAHITI	Database for Hydrological Time Series of Inland Waters	UCM	User Consultation Meeting
DEM	Digital Elevation Model	WP	Work Package
DTU	Technical University of Denmark	WSH	Water Surface Height
EO	Earth Observation		
ERR	Evolutions Recommendation Report		
ESA	European Space Agency		
FIS	Finnish Ice Service		
FMI	Finnish Meteorological Institute		
FRAPPE	Flexible Radar Altimeter Processor for Performance Evaluation		
FRM4ALT	Fiducial Reference Measurement for Altimetry		
FRD4ALT	Fundamental Data Records for Altimetry		
G-REALM	Global Reservoirs and Lakes Monitor		
GDR	Geophysical Data Records		
GLWD	Global Lakes and Wetlands Database		
GSWE	Global Surface Water Explorer		
IMEDEA	Instituto Mediterráneo de Estudios Avanzados		
IPCC	Intergovernmental Panel on Climate Change		
IRPI	Istituto di Ricerca per la Protezione Idrogeologica		
ISRO	Indian Space Research Organisation		
ITT	Invitation To Tender		
JPL	Jet Propulsion Laboratory		
LEGOS	Laboratoire d'Étude en Géophysique et Océanographie Spatiale		
LRM	Low Resolution Mode		
LU	Lancaster University		
MDT	Mean Dynamic Topography		
MSS	Mean Sea Surface		
MSSL	Mullard Space Science Laboratory (part of UCL)		
NCR	Non Conformance Report		
NERSC	Nansen Environmental and Remote Sensing Center		
OCOG	Offset Centre Of Gravity retracker		
PDS	Payload Data Segment		
PEG	Polar Expert Group		
PM	Project Manager		
PO	Polar Oceans		
PSMSL	Permanent Service for Mean Sea Level		

RA	Radar Altimeter / Altimetry		
----	-----------------------------	--	--

TABLE OF CONTENTS

1	<i>Introduction</i>	5
1.1	Purpose and Scope.....	5
1.2	Document Structure.....	5
1.3	Applicable and Reference Documents.....	6
	Applicable documents	6
	Reference documents.....	6
2	<i>Inland Water Parameters</i>	7
2.1	Parameter Definition	7
2.2	Target Audience and Intended Use	8
3	<i>Overall Inland Water Processing Flow</i>	8
4	<i>Algorithm Description</i>	9
4.1	Input Data	9
4.2	Selection and editing.....	9
4.3	Water Surface Height Estimation	11
4.3.1	Propagation and Geophysical Corrections	12
4.3.2	Range	13
4.4	Quality Flag	15
4.5	Uncertainty.....	18
4.6	Ancillary data.....	18
5	<i>Limitations and Known Issues</i>	19
6	<i>References</i>	19

1 Introduction

1.1 Purpose and Scope

This document comprises the Algorithm Theoretical Basis (ATBD) for the inland water algorithm used for the *CryoSat-2 ThEMatic PrOducts (Cryo-TEMPO)* study, Ref: ESA AO/1-10244/2-/I-NS. The ATBD has been written by the Inland Water team led by CLS, with contributions from all members of the Cryo-TEMPO consortium. Lancaster University as the prime contractor is the contact point for all communications regarding this document.

1.2 Document Structure

This document covers the description of algorithms to estimate the inland water level at level 2 for wide variety of users. The document is structured as follows:

- Section 1 – Introduction
- Section 2 – Inland Water Parameters
- Section 3 – Overall Inland Waters Processing Flow
- Section 4 – Algorithm Descriptions
- Section 5 – Limitations and Known Issues

1.3 Applicable and Reference Documents

Applicable documents

Reference	Title
AD1	Statement of Work ESA Express Procurement Plus - EXPRO+ CryoSat-2 ThEMatic PrOducts Cryo-TEMPO, Issue 1, Revision 0, Date of Issue 01/04/2020 [Ref. ESA-EOPG-EOPGMQ-SOW-10].
AD2	Invitation to Tender for CryoSat-2 ThEMatic PrOducts Cryo-TEMPO REF.: ESA AO/1-10244/2-/I-NS [Ref. SA-IPL-POE-NS-sp-LE-2020-313].
AD3	Draft Contract, CryoSat-2 ThEMatic PrOducts Cryo-TEMPO, Appendix 2 to ESA AO/1-10244/20/I-NS.

Reference documents

Reference	Title
RD1	Copernicus Polar and Snow Cover Applications User Requirements Workshop, http://www.copernicus.eu/polar-snow-workshop
RD2	PEG-1 Report, User Requirements for a Copernicus Polar Mission, Step 1 Report, Polar Expert Group, Issue: 12th June 2017
RD3	PEG-2 Report, Polar Expert Group, Phase 2 Report on Users Requirements, Issue: 31st July 2017
RD4	Baseline-C CryoSat-2 Ocean Processor, Ocean Product handbook. Version 4.1 (https://earth.esa.int/documents/10174/125272/CryoSat-Baseline-C-Ocean-Product-Handbook)

2 Inland Water Parameters

The Cryo-TEMPO Inland Water product contains the water surface height with respect to the geoid (Figure 1).

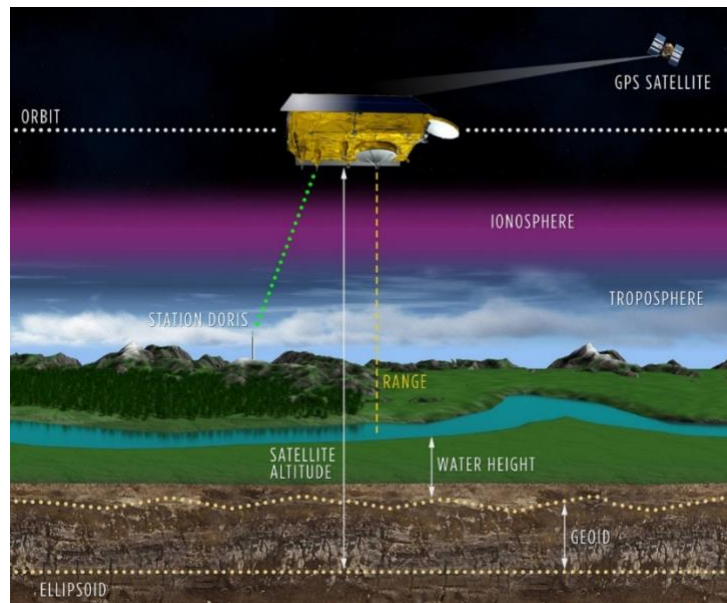


Figure 1. Schematic of the principle to retrieve surface water height from altimeter observations.

2.1 Parameter Definition

Cryo-Tempo Inland Water products contain measurements along track (20Hz) of the CryoSat-2 orbit for locations with a water occurrence above zero according to Global Surface Water Explorer, that provides statistics from 1984 to 2018. Table 1 contains the main parameters contained in the Inland Water products.

Table 1. Main parameter in Inland Water Products

Parameter	Description	Units
Latitude	Latitude of estimated echo location	Degrees North
Longitude	Longitude of estimated echo location	Degrees East
Water Surface Height	Estimated water surface height with respect to the ellipsoid all instrumental and geophysical corrections applied	m

Measurement mode	The mode the CryoSat SIRAL instrument was in when each measurement was taken (LRM, SAR)	flag
Geoid	Geoid above reference ellipsoid from Earth Gravitational Model EGM 2008	m
Uncertainty	Uncertainty of the measurement	m
Quality flag	Flag indicating the validity of the measurement	flag
Land Water occurrence	Percent of water occurrence based on Global Surface Water Explorer dataset	percent
Surface type	Type of the surface based on Global Lakes and Wetlands Database (GLWD3)	No units

2.2 Target Audience and Intended Use

The target audience for Cryo-TEMPO thematic inland water product are satellite altimetry expert and non-expert users who require access to surface water level observations from CryoSat-2 at full resolution and with processing steps and assumptions specific for the inland waters.

3 Overall Inland Water Processing Flow

The processing flow for generating the inland water level products consists of 4-steps (Figure 2):

- **Selection** of the measurements on land and definition of the flag values (a process called **editing**) depending on the retracker.
- Estimation of the water level: in this step, the **geophysical corrections** are applied: Dry tropospheric, Wet tropospheric, Ionospheric, Earth tides and polar tides.
- Addition of the **quality flag** and the **uncertainty**.
- Include **ancillary data**: surface type and water occurrence. Only measurements with water occurrence above zero (GSWE) are provided.

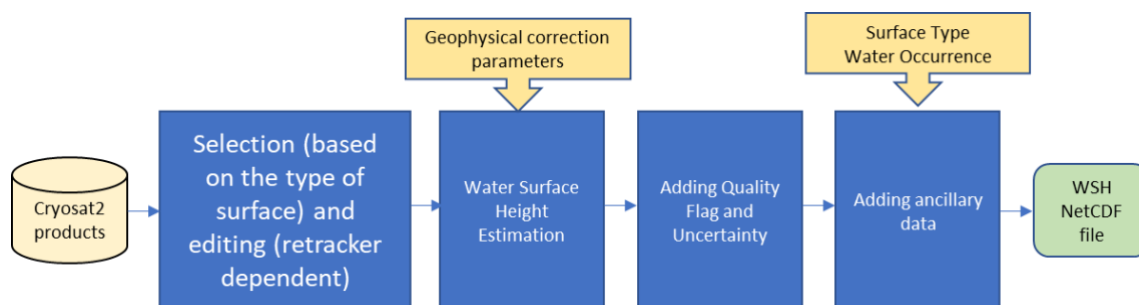


Figure 2. Overview of the processing chain for inland waters.

The different subprocess are described in the following sections.

4 Algorithm Description

Satellite altimeters are designed to measure the two-way travel time of short radar (or laser) pulses reflected from the Earth’s surface which gives the distance between the satellite and the reflected surface, called “range” (Figure 1Error! Reference source not found.).

4.1 Input Data

Primary input data for the Cryo-TEMPO thematic inland water product is Level-2 data from the ESA CryoSat-2 baseline-C GOP processing chain for LRM, SAR and SARIn modes. The files are delivered as one netCDF file separated by changes of the radar mode. Information about the CryoSat-2 products of the GOP processor can be found in RD4.

4.2 Selection and editing

A first selection for inland water products consists in keeping only those points that are not in open ocean based on the surface type flag provided in the CryoSat-2 products.

The second editing is based on the backscatter coefficient value (σ_0) and is retracker dependent. Three different retracker (MLE4, OCOG and TFMRA) are included in the Cryo-TEMPO phase-1 TDS. A single retracker will be selected following validation study of the TDS. According to previous analysis, based on the statistics behaviour, the σ_0 thresholds to be applied per retracker are listed in Table 2. Figures 5-7, show the behaviour of the σ_0 over an Envisat cycle for different surface types based on GLWD3: lakes and reservoirs in red, rivers in blue, flood plains in grey and wetlands in green and justify the editing thresholds employed.

Table 2. Threshold of σ_0 per retracker.

Retracker	MLE4	OCOG	TFMRA
Threshold	7dB	5 dB	8 dB

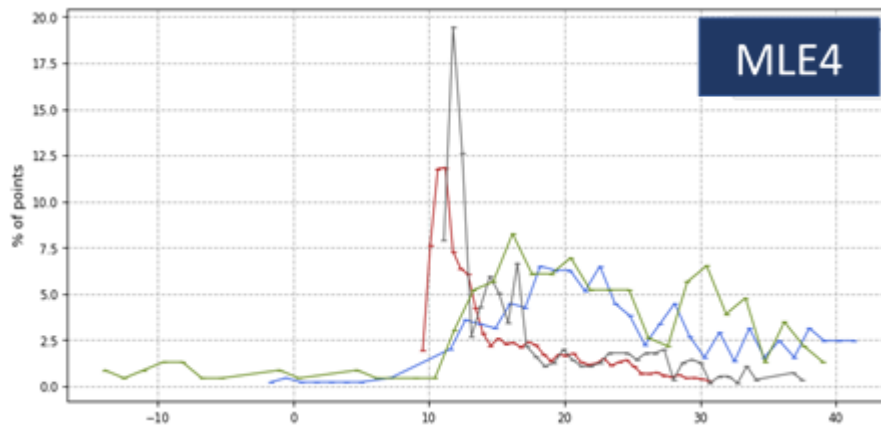


Figure 5. MLE4 retracker: Sigma0 behaviour.

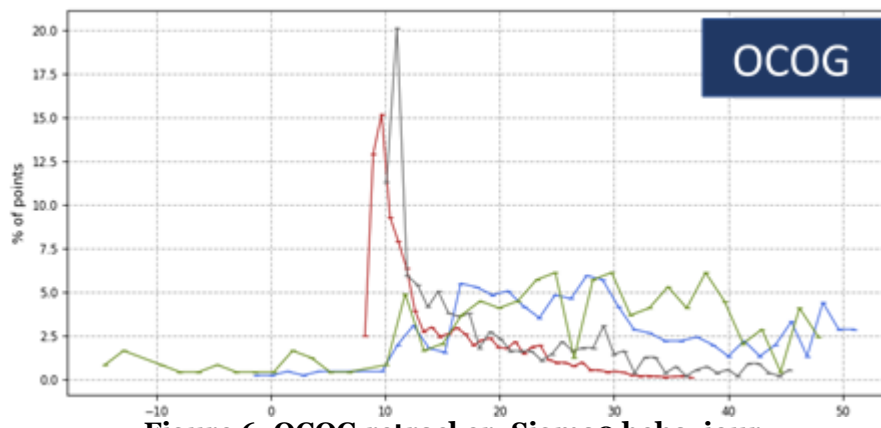


Figure 6. OCOG retracker: Sigma0 behaviour

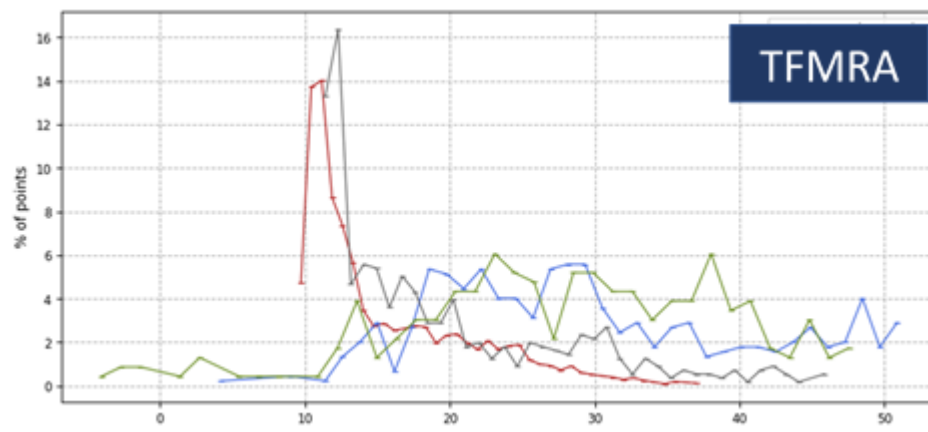


Figure 7. TFMRA retracker: Sigma0 behaviour

4.3 Water Surface Height Estimation

Radar altimeters send an electromagnetic pulse to the satellite nadir and record the propagation time to and from the emitted wave and its echo from the surface. The electromagnetic bands of interest are the Ku and Ka bands, which are reflected perfectly – without penetration – by water (which is not the case for snow). Multiplied by the speed of light c , half the time it takes for the transmission it gives length R (the range) between the satellite and the reflective surface:

$$R = c \frac{\Delta t}{2} \quad [3.1]$$

The height H of the reflective surface is given by the following equation:

$$H = a - (R + \Sigma C_p + \Sigma C_g) \quad [3.2]$$

where a is the orbital altitude of the satellite with respect to the ellipsoid. Corrections must be made for propagation in the atmosphere (C_p) and also vertical movements of Earth's crust (C_g).

The ellipsoidal height is then converted into elevation h , taking the local undulation of geoid N into account:

$$h = H - N \quad [3.3]$$

The ΣC_p and ΣC_g terms in Equation 3.2 correspond to sets of corrections that must be subtracted to obtain an accurate estimation of H .

There are two types of corrections:

- propagation corrections (C_p) needed because the radar pulse propagates through the atmosphere at a speed below the speed of light c used in Eq. 3.1
- geophysical corrections (C_g) linked to the vertical movements of the Earth surface (tides, for example) and for which we want to correct the measurement in order to apply it to a fixed geodetic datum in the terrestrial reference frame.

Finally, we can express the height of a lake by the full following equation:

$$h = a - R - DTC - WTC - IC - ET - PT - LT - SSB-N \quad [3.4]$$

where DTC is the dry tropospheric correction, WTC the wet tropospheric correction, IC the ionospheric correction, ET the Earth tide, PT the pole tide, LT the lake tide and SSB the instrumental so-called sea state bias. Lake tide LT and SSB are not considered in our calculation since they are minor compared to other corrections. Similarly, the ocean loading is not included in the equation because it has very little impact on inland waters.

The term N in Eq's. 3.3 and 3.4 corresponds to the geoid correction that must be applied to each altimetry measurement and is also provided in the product.

4.3.1 Propagation and Geophysical Corrections

Several geophysical and propagation corrections need to be applied to the altimeter range to get precise water level height. These are described in turn below.

DTC is directly proportional to the atmospheric pressure and it is given by the Geophysical Data Records (GDR). The altitude of the lake is taken into account for the atmospheric pressure used in the calculation.

WTC is related to the water vapor contained in the air column that the electromagnetic wave intersects. This correction can be estimated in two ways: either with an onboard bi- or tri-frequency radiometer or from a global meteorological model, as used for dry tropospheric correction. It has been pointed out that the correction using a radiometer is highly erroneous over continental water or coastal regions, due to land contamination, up to a distance of 20 to 30 km from the coastline. Therefore, apart from very large lakes, the WTC used in continental water comes directly from a model based on climate gridded data sets of multi-layer water vapour and temperature fields based on the ECMWF. WTC varies geographically and seasonally and can amount to several decimetres. The WTC model also takes lake altitude into account.

The **IC** correction is related to the interaction of the electromagnetic wave with free electrons in the upper atmosphere. It is proportional to the Total Electronic Content (TEC) in this layer of the atmosphere and inversely proportional to the square of the pulse frequency. It has been shown that over lakes, this correction could be erroneous due to land contamination if the measurement is taken close to the shoreline. Therefore, it may be preferable to use the IC derived from the Global Ionospheric Maps (GIM), inferred from the GNSS worldwide network. This correction is directly available from the CryoSat-2 baseline-C GOP (RD4).

The Earth tide (**ET**) and Pole tide (**PT**) are estimated using models and are provided within the GDRs. PT is related to changes in centrifugal forces, and thus the flattened shape of the Earth, by variations created through fluctuations in the rotational axis of the Earth. The vertical movements of the surface of the Earth associated with this tide are at the centimetre level and are well modelled. ET is linked to astronomical gravitational forces surrounding the Earth, essentially variations in lunar and solar attraction based on their position in the space. The vertical movements of the surface of the Earth related to the ET are around twenty centimetres.

Therefore, in Inland Water products it is most appropriate to apply corrections from models. Table 3 includes the sources of the models used in the water eight estimation in the Inland Water product.

Table 3. Geophysical correction models used in Inland Water estimation.

Geophysical Correction	Description	Source
Dry Troposphere (DTC)	Correction for refraction due to the dry gas component of the atmosphere	ECMWF
Wet Troposphere (WTC)	Correction for the path delay due to water vapor in the atmosphere	ECMWF
Ionosphere (IC)	Correction for the free electrons in the Earth's ionosphere	GIM
Solid earth tide (ET)	Correction for the deformation of earth's body due to tidal forces	Cartwright
Pole tide (PT)	Correction for the long period	Desai 2015 with 2017 mean pole location

4.3.2 Range

The shape of the reflected signal, known as the “waveform”, represents the power distribution of accumulated echoes as the radar pulse hits the surface. The so-called onboard tracking system is the software which attempts to keep the reflected radar echo within the receiver observation window. The resulting waveforms are called ‘tracked waveforms’. The satellite range can be derived from this waveforms by a process called retracking. The first altimetry missions were designed for the ocean domain and the corresponding retracking consisted in fitting an analytical function, the so-called Brown model (Brown 1977) to the echoes reflected by ocean surfaces. This model considers that thermal noise is followed by a rapid rise of the returned power called ‘leading edge’, and a gentle end sloping plateau known as ‘trailing edge’. However, over the continents the waveforms are generally contaminated by noise resulting from multiple land returns such as vegetation, bare sands, or steep shorelines. Consequently, the shape of the echoes reflected by continental waters is often very different from that reflected by the ocean surface. It can thus become difficult, if not impossible, to calculate the water level of a river or small lake using the classic Brown analytic function. One way of working around this is to use alternative and more suitable re-tracking methods of the waveforms. Different retracking algorithms, are used to calculate the range: MLE4, OCOG and TFMRA. These are described in turn below.

MLE4:

Over big lakes, similar to ocean surfaces, the radar waveform has a characteristic shape than can be described analytically, in both Low Resolution Mode (LRM) (Brown et al., 1977; Hayne et al., 1980) and Synthetic Aperture Radar (SAR) mode (Halimi et al., 2014; Dinardo et al., 2015). Three main geophysical parameters act on the waveform shape and position in the window analysis: sea surface height, significant wave height and backscattering energy (Sigma-0). An unweighted least square estimate derived from a Maximum Likelihood Estimator (MLE) is available in CryoSat-2 baseline-C GOP product (RD4).

Ice OCOG:

Over heterogenous or non-flat surfaces analytical and theoretical models are no longer valid. Empirical methods are generally employed to derive the surface topography from the altimetry waveforms. The Offset Centre Of Gravity retracker (OCOG) algorithm was first introduced by Wingham et al. (1986). It is a purely statistical approach with the aim to estimate different shape parameters in the waveform, in particular its amplitude (A) and centre of gravity (COG). In the ICE-1 method, the retracking point is obtained by interpolation between the first samples that crosses the power threshold $t \cdot A$, with t a threshold between 0 and 1. Through the retracking point, referred as “epoch” parameter, the surface topography can be estimated. Range from this retracker is also available in CryoSat-2 baseline-C GOP product (RD4).

TFMRA:

More recently Helm et al. (2014) adapted the OCOG/ICE-1 retracker in order to estimate the retracking point on the first waveform leading edge, theoretically corresponding to Point Of Closest Approach: the Threshold First Maximum Retracker (TFMRA) that was also applied for the three acquisition modes. It ties the main scattering horizon at a certain threshold of the first maximum peak power of the waveform, considering the noise floor. Over inland waters this means that the retracker objective is to estimate the surface topography for the water body the closest to the satellite, within the radar footprint. The current threshold for SAR/SARin acquisition mode is 80 % and for LRM/PLRM the threshold is 25%.

The Threshold First Maximum Retracking Algorithm (TFMRA) version used for the Cryo-TEMPO project was developed in house by CLS. The implementation follows closely the initial definition made by Helm et al. (2014). The only noticeable difference is on the first peak detection, an alternative approach was chosen with the objective to be less sensitive to speckle noise in the first local maxima/peak research (in Helm et al. [2014] a 3-point Lagrangian interpolation is employed). This TFMRA version was used with success for studying CryoSat-2 SAR & PLRM measurements over Antarctica (Aublanc et al., 2018).

The algorithm, briefly summarized below, includes the following computational steps:

- Waveform (*WF*) normalization by its maximum energy
- Thermal noise computation (*thn*) using the first range bins (averaged energy between gates $N=4$ and $N=10$)
- Waveform oversampling by a factor of 10 using linear interpolation
- Computation of a smoothed waveform with a boxcar average of width 15 oversampled gates
- First peak detection:
 - Loop over the waveform nominal gates
 - Polynomial fitting on the oversampled smoothed waveform (over +/- 50 oversampled gates)
 - If the first order of the fitted function is negative, a peak is potentially detected, and its maximal value is temporarily stored (*Pmax1*)
 - The first peak is reached if an energy decrease is observed on $N=5$ successive nominal gates, and if the maximal energy of the detected peak exceeds 33% of *WF* maximal value + *thn* value ($0.33+thn$)
- Determination of the first gate *N* exceeding the threshold level (*TL*) at the leading edge of the first detected peak, where " $N > Pmax1 \times TL + thn$ ". In case of no peak detection, *Pmax1* corresponds to "1", the maximal value of the normalized *WF*.
- The epoch position is computed by linear interpolation between adjacent oversampled bins to the threshold crossing

4.4 Quality Flag

The quality flag included in the inland water products indicates the confidence that can be attributed to the measurement. In the case of inland waters, the quality flag depends on the acquisition mode and on the shape of the echo waveform. At CLS, we have used machine learning algorithm to classify the SAR waveforms in 20 categories (Poisson et al, 2018). Currently, this classification is available for measurements in LRM and SAR mode. The waveform classification is dependent on the acquisition mode, and some waveform classes are not used for LRM. The three groups for LRM are shown in Figure 3 (reliable) and Figure 4 (disturbed and unreliable). For the SAR acquisition mode, the three groups are shown in **Error! Reference source not found.**, **Error! Reference source not found.** and **Error! Reference source not found.** for reliable, disturbed and unreliable waveforms. For LRM and SAR modes, there are two different levels of quality depending on the classification of the wave form: level 0, the best level for waveforms in group 1 and 2 (reliable and disturbed waveforms) and level 2 for poor quality measurements belonging to the unreliable group waveforms.

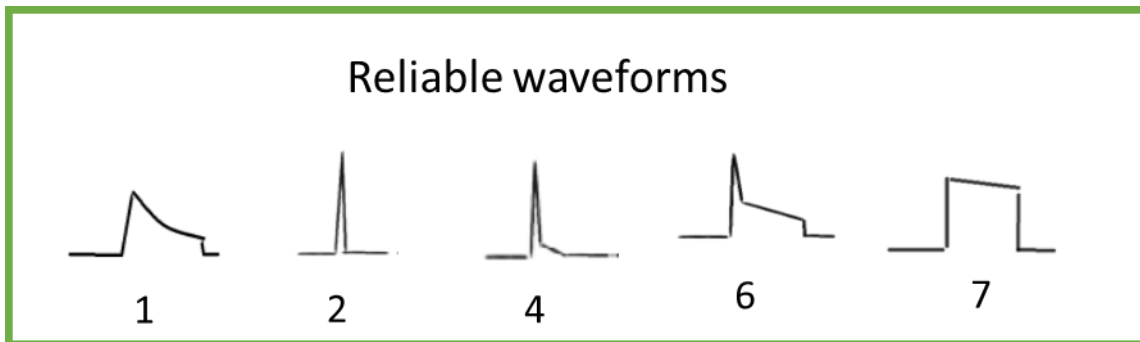


Figure 3. Group 1: LRM reliable waveforms.

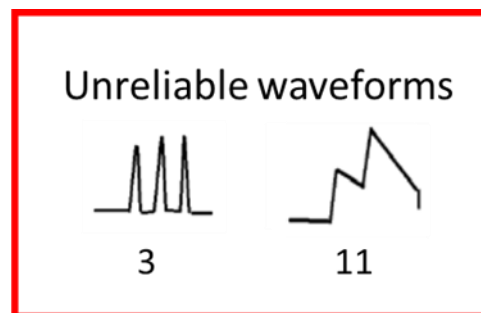
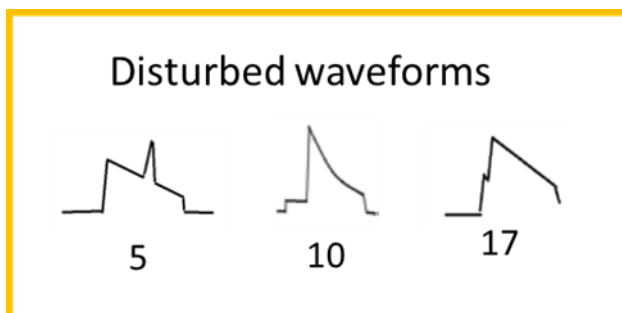


Figure 4. Groups 2 and 3: LRM disturbed and unreliable waveforms.

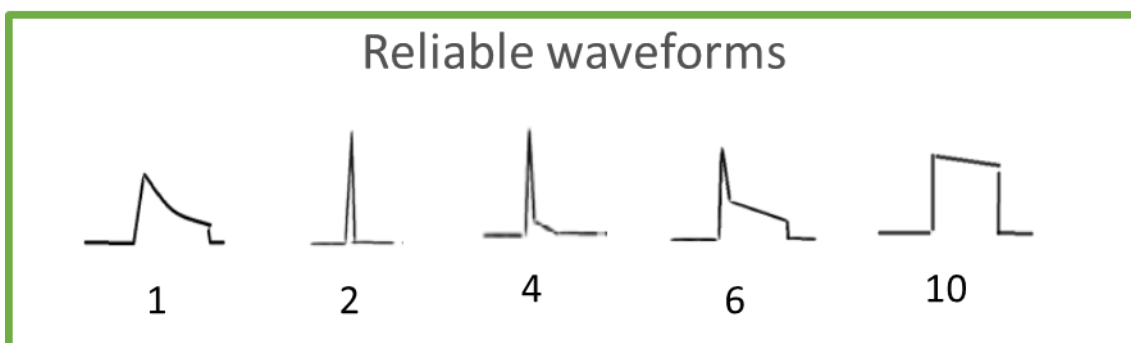


Figure 5. Group 1: SAR reliable waveforms

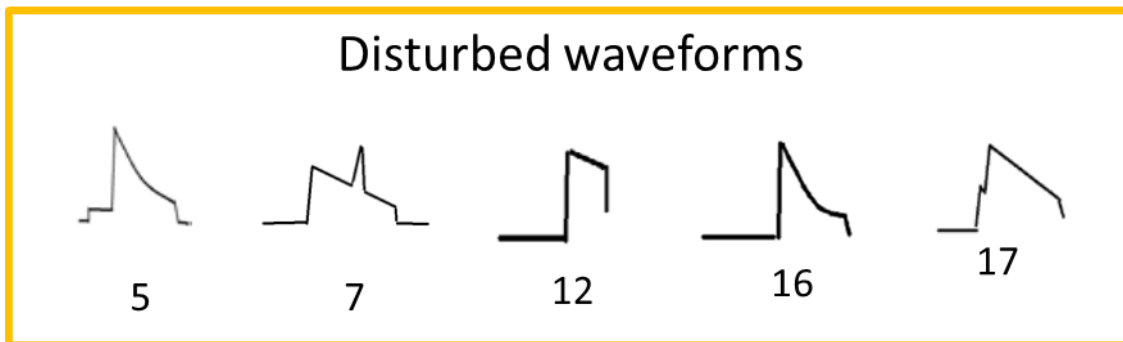


Figure 6. Group 2: SAR disturbed waveforms

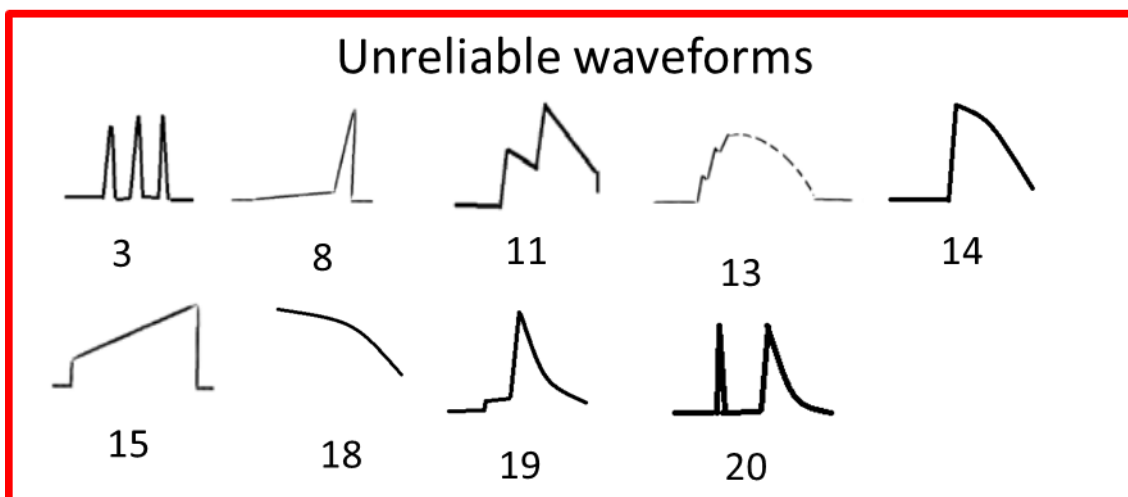


Figure 7. Group3: SAR unreliable waveforms.

Machine learning algorithm to classify SARin waveforms has not been implemented, therefore other approach needs to be performed to define a quality flag for this third acquisition mode. To do so, we systematically evaluate the quality measurement based on the complexity of the SARin waveforms, and more particularly on its number of peaks. A data is considered as bad quality measurement (level 2) if the waveform is “multipeak”, while good quality measurement (level 0) corresponds to “unipeak” waveform. A waveform is defined as “multipeak” if there is at least one peak with an amplitude higher than 40% and separated by more than 30 gates of the maximum peak of the waveform. These values of % relative to the maximum amplitude and number of gates have been tuned on a study case (Lake Athabasca) to optimize the amount of good quality measurement and the value of the standard deviation for WSH.

4.5 Uncertainty

The uncertainty, still under evaluation, will be based on the FDR4ALT methodology. It implies to provide bottom-up estimation based on statistical analysis per acquisition mode (LRM, SAR, SARIn), retracking (MLE4, OCOG, TFMRA) and surface type (based on GLWD3 classification). The uncertainty, provided along track in the inland water products, is given by the quadratic sum of the uncertainties from each component of water surface height (equation 3.4). Regarding the geophysical uncertainties, Table 4 summarises the uncertainty values of the different models used for the estimation of the water surface height based on literature (Fernandes 2014, Cretaux 2009, Birkett and Beckley 2010).

Table 4. Geophysical uncertainties for inland water

Correction	Uncertainty (cm)
DCT (ECMWF)	0.3
WTC (CEMWF)	3
IC (GIM)	2
ET (Cartwright)	0.3
PT (Desai)	0.3

The errors in the geophysical correction are small compared to errors related to retracking and potential biases introduced by empirical retrackers (Vieira et al, 2018). Nevertheless, they are important to obtain accurate absolute water levels. The uncertainty on the range is specific to each retracking algorithm, it will be estimated empirically as the median of all the differences in between two consecutive measurements during a complete CryoSat-2 cycle (369 days) belonging to a certain group. As mentioned above, the groups will be created as a function of the retracking algorithm and also of the acquisition mode and the type of surface.

4.6 Ancillary data

Two ancillary data sets are included in the product to provide useful information to the users: the type of the surface based Global Lakes and Wetland Database (GLWD) and the water occurrence from Global Surface Water Explorer (GSWE). Table 5 **Error! Reference source not found.** contains the main characteristics of these datasets.

Table 5. Characteristics of ancillary data for inland water product.

GSWE	Data contents	Percent of water occurrence
	Data source	Global Surface Water Explorer
	Resolution	30 m
GLWD3	Data contents	Type of the surface

	Data source	Global lakes and Wetlands Database
	Resolution	30 arc sec

5 Limitations and Known Issues

The inland water product implemented in the first phase of the Cryo-TEMPO project contains the water surface height from three retrackerers. Two of them use data directly from Cryosat-2 Ocean processing Baseline C: OCOG and MLE4 algorithms (in PLRM mode if the acquisition mode is SAR or SARIn), while the third retracker algorithm, TFMRA, has been made available for the three acquisition modes. As the thresholds used to set this algorithm have been set over ocean surfaces, it may not be the most appropriate for inland waters, making an adjustment necessary in future versions of the TDP.

Furthermore, in the CryoSat-2 Ice processing Baseline D, a hamming window is generated once at the beginning of the SAR processing and applied in the azimuth direction, to all echoes of every burst at the very beginning of the beam-forming step (RD5). This process is probably more adapted to inland water targets and deserves to be analysed during the further phases of the project.

An additional retracker will be also evaluated: SAMOSA+ (Dinardo et A, 2018). This physical retracker will be considered to provide a better range estimation by limiting the impact of land contamination.

6 References

Aublanc, J., Moreau, T., Thibaut, P., Boy, F., Rémy, F. and Picot, N.: Evaluation of SAR altimetry over the antarctic ice sheet from CryoSat-2 acquisitions, *Advances in Space Research*, 62(6), 1307–1323, doi:10.1016/j.asr.2018.06.043, 2018.

Birkett C. M. (1995). Contribution of TOPEX/POSEIDON to the global monitoring of climatically sensitive lakes, *Journal of Geophysical Research*, 100, C12, 25, 179-25, 204

Birkett, C.M. and Beckley, B. (2010) Investigating the Performance of the Jason-2/ OSTM Radar Altimeter over Lakes and Reservoirs. *Marine Geodesy*, 33, 204-238.

Birkett, C.; Reynolds, C.; Beckley, B.; Doorn, B. From Research to Operations: The USDA Global Reservoir and Lake Monitor. In *Coastal Altimetry*; Vignudelli, S., Kostianoy, A.G., Cipollini, P., Benveniste, J., Eds.; Springer-Verlag: Berlin/Heidelberg, Germany, 2011; pp. 19–50.

Brown G. S. (1977). The Average Impulse Response of a rough surface and its applications, *IEEE Trans. Antennas Propag*, Vol. 25, pp. 67-74. 10.1109/TAP.1977.1141536

Crétaux J-F. and Birkett C. M. (2006). Lake studies from satellite altimetry, *C R Geoscience*, 10.1016/J.crte.2006.08.002

Crétaux, JF., Calmant, S., Romanovski, V. et al. An absolute calibration site for radar altimeters in the continental domain: Lake Issykkul in Central Asia. *J Geod* 83, 723–735 (2009). <https://doi.org/10.1007/s00190-008-0289-7>

Crétaux J-F. Calmant S. Romanovski V. Perosanz F. Tashbaeva S. Bonnefond P. Moreira D. Shum C. K. Nino F. Bergé-Nguyen M. Fleury S. Gegout P. Abarca Del Rio R. Maisongrande P. (2011). Absolute Calibration of Jason radar altimeters from GPS kinematic campaigns over Lake Issykkul, *Marine Geodesy*, 34: 3-4, 291-318, 10.080/01490419.2011.585110

Cretaux J-F, Abarca Del Rio R. Berge-Nguyen M. Arsen A. Drolon V. Clos G. Maisongrande P. 2016. Lake volume monitoring from Space, *Survey in geophysics*, 37: 269-305. 10.1007/s10712-016-9362-6

Cretaux J-F. Bergé-Nguyen M. Calmant S. Jamangulova N. Satylkanov R. Lyard F. Perosanz F. Verron J. Montazem A. S. Leguilcher G. Leroux D. Barrie J. Maisongrande P. and Bonnefond P. (2018). Absolute calibration / validation of the altimeters on Sentinel-3A and Jason-3 over the lake Issykkul, *Remote sensing*, 10, 1679. 10.3390/rs10111679

Dinardo S. et al.: Coastal SAR and PLRM altimetry in German Bight and West Baltic Sea, *Advances in Space Research* 2018.

Fernandes, M. J.; Lázaro, Clara; Nunes, Alexandra L.; Scharroo, Remko. 2014. "Atmospheric Corrections for Altimetry Studies over Inland Water" *Remote Sens.* 6, no. 6: 4952-4997. <https://doi.org/10.3390/rs6064952>

Halimi, A., Mailhes, C., Tournet, J.-Y., Thibaut, P. & Boy, F. A Semi-Analytical Model for Delay/Doppler Altimetry and Its Estimation Algorithm. *IEEE Transactions on Geoscience and Remote Sensing* 52, 4248–4258 (2014).

Hayne, G. Radar altimeter mean return waveforms from near-normal-incidence ocean surface scattering. *IEEE Transactions on Antennas and Propagation* 28, 687–692 (1980).

Helm, V., Humbert, A. & Miller, H. Elevation and elevation change of Greenland and Antarctica derived from CryoSat-2. *The Cryosphere* 8, 1539–1559 (2014).

Poisson, J.C et al.: "Development of an ENVISAT altimetry processor providing sea level continuity between open ocean and Arctic leads", *IEEE Transac of Geoscience & Remote Sensing*, 2018.

Ričko M. C. M. Birkett, J. A. Carton, and J-F. Cretaux. (2012). Intercomparison and validation of continental water level products derived from satellite radar altimetry, *J. of Applied Rem. Sensing*, Volume 6, Art N°: 061710.10.1117/1.JRS.6.061710

Telmo Vieira, M. Joana Fernandes, Clara Lázaro, Analysis and retrieval of tropospheric corrections for CryoSat-2 over inland waters, *Advances in Space Research*, Volume 62, Issue 6, 2018. <https://doi.org/10.1016/j.asr.2017.09.002>.



Wingham, D., Rapley, C. & Griffiths, H. NEW TECHNIQUES IN SATELLITE ALTIMETER TRACKING SYSTEMS. <https://www.semanticscholar.org/paper/NEW-TECHNIQUES-IN-SATELLITE-ALTIMETER-TRACKING-Wingham-Rapley/1bb8b81c9fb0d7f57dc602fe3b2f401fd359902d> (1986)